



**Table 1.** Crystallographic Data for Compounds  $[\text{Pr}_2\text{NPP}(\text{SiMe}_3)_2]_2 \cdot \text{Fe}(\text{CO})_4$  (**4**) and  $[(\text{tBuNP})_2\text{P}(\text{SiMe}_3)_2]_2$  (**11**)

	<b>4</b>	<b>11</b>
empirical formula	$\text{C}_{22}\text{H}_{46}\text{N}_2\text{O}_4\text{Si}_2\text{P}_4\text{Fe}$	$\text{C}_{22}\text{H}_{54}\text{N}_4\text{P}_6\text{Si}_2$
fw	638.5	616.7
$a$ , Å	11.744(2)	9.977(2)
$b$ , Å	19.138(4)	11.087(3)
$c$ , Å	15.613(3)	18.542(5)
$\alpha$ , deg	90	89.13(2)
$\beta$ , deg	94.715(13)	82.97(2)
$\gamma$ , deg	90	64.01(2)
$V$ , Å <sup>3</sup>	3497.0(11)	1828.2(8)
$\lambda$ , Å	0.71069	0.71073
space group	$P2_1/n$	$P1$
$Z$	4	2
$D(\text{calcd})$ , g cm <sup>-3</sup>	1.213	1.120
$t$ , °C	293	293
$\mu$ , cm <sup>-1</sup>	7.04	3.70
transm factors	0.2875/0.3266	0.8903/0.9494
$R(F)^a$	7.23	6.48
$Rw(F^2)^b$	6.62	6.20

<sup>a</sup>  $R(F) = \sum(|F_o| - |F_c|)/\sum|F_o|$ . <sup>b</sup>  $Rw(F^2) = [\sum w(|F_o| - |F_c|)^2 / \sum wF_o^2]^{1/2}$ .

hexane (50 mL) was combined with  $(\text{Me}_3\text{Si})_2\text{PLi} \cdot 2\text{THF}$  (1.6 g, 4.8 mmol) at  $-78^\circ\text{C}$ . The mixture was stirred at  $-78^\circ\text{C}$  (2 h) and  $23^\circ\text{C}$  (16 h) and filtered, and the filtrate was concentrated to  $\sim 5$  mL whereupon a yellow crystalline solid (**10**) deposited at  $-10^\circ\text{C}$ : yield, 1.1 g (81%); mp  $100\text{--}103^\circ\text{C}$ . Mass spectrum (30 eV) [ $m/e$  (%): 381 (100). Infrared spectrum (hexane,  $\text{cm}^{-1}$ ): 1364 (w), 1244 (m), 1215 (w), 1198 (s), 962 (w), 835 (vs), 745 (w), 627 (w). Anal. Calcd for  $\text{C}_{20}\text{H}_{54}\text{N}_2\text{Si}_4\text{P}_4$  (558.92): C, 42.98; H, 9.74; N, 6.01. Found: C, 43.22; H, 10.08; N, 5.08.

**Synthesis of Cage Derivative (11).** A sample of  $(\text{tBuNPLi})_2$  (1.5 g, 5.4 mmol) in hexane (100 mL) was cooled to  $-78^\circ\text{C}$  and  $(\text{Me}_3\text{Si})_2\text{PLi} \cdot 2\text{THF}$  (1.8 g, 5.4 mmol) was added slowly in portions as a solid reagent. The mixture was stirred (3 h), warmed to  $23^\circ\text{C}$ , and stirred (16 h). The cloudy, orange solution was filtered and the filtrate concentrated to  $\sim 10$  mL. Orange crystals of **11** deposited at  $-10^\circ\text{C}$ : yield 0.4 g (24%); mp  $173\text{--}176^\circ\text{C}$  (dec). Mass spectrum (30 eV) [ $m/e$  (%): 616 ( $\text{M}^+$ , 1.7), 412 (6), 235 (100). Infrared spectrum (hexane,  $\text{cm}^{-1}$ ): 1379 (w), 1364 (m), 1253 (m), 1246 (m), 1218 (m), 1071 (w), 1041 (w), 1009 (w), 984 (w), 953 (w), 927 (w), 917 (w), 895 (w), 879 (m), 840 (vs), 763 (w), 754 (w), 628 (w), 509 (w). Anal. Calcd for  $\text{C}_{22}\text{H}_{54}\text{N}_4\text{Si}_2\text{P}_6$  (616.72): C, 42.85; H, 8.82; N, 9.08. Found: C, 42.18; H, 9.03; N, 8.82.

**1,4-Bis(trimethylsilyl)phosphido-2,3,5,6-tetramethyl-2,3,5,6,1,4-tetrazadiphosphetidine (9).** A sample of  $\text{ClP}(\text{MeN})_4\text{PCL}$  (0.5 g, 2.0 mmol) in hexane (50 mL) was cooled to  $-78^\circ\text{C}$  and  $(\text{Me}_3\text{Si})_2\text{PLi} \cdot 2\text{THF}$  (1.3 g, 4.0 mmol) was cooled to  $-78^\circ\text{C}$  and  $(\text{Me}_3\text{Si})_2\text{PLi} \cdot 2\text{THF}$  (1.3 g, 4.0 mmol) was added slowly in portions as a solid reagent with stirring. The mixture was stirred at  $-78^\circ\text{C}$  and (2 h) and then at  $23^\circ\text{C}$  (16 h) and filtered, and the filtrate evaporated to dryness. The residue was recrystallized from hexane ( $-10^\circ\text{C}$ ) leaving colorless crystals (**9**): yield, 0.65 g (61%); mp  $234\text{--}236^\circ\text{C}$ . Mass spectrum (30 eV) [ $m/e$  (%): 355 (55). Infrared spectrum (hexane,  $\text{cm}^{-1}$ ): 1246 (m), 1082 (w), 1067 (w), 932 (w), 839 (s), 779 (w), 756 (w), 731 (w), 627 (w), 484 (w), 468 (w). Anal. Calcd for  $\text{C}_{16}\text{H}_{48}\text{N}_4\text{Si}_4\text{P}_4$  (532.83): C, 36.07; H, 9.08; N, 10.52. Found: C, 35.94; H, 9.38; N, 10.40.

**Crystallographic Measurements and Structure Solutions.** Crystals of **4** and **11** were placed in glass capillaries under a dry nitrogen atmosphere. The crystals were centered on a Siemens R3m/V automated diffractometer and determinations of crystal class, orientation matrix, and unit cell dimensions were performed in a standard manner. Selected crystallographic data are summarized in Table 1. Data were collected in the  $2\theta$  scan mode with Mo  $K\alpha$  radiation, a scintillation counter, and pulse height analyzer. Inspection of a small data set led to assignment of the space groups.<sup>10</sup> Semi-empirical adsorption corrections were applied based on  $\psi$  scans.<sup>11</sup> No signs of crystal decay were noted.

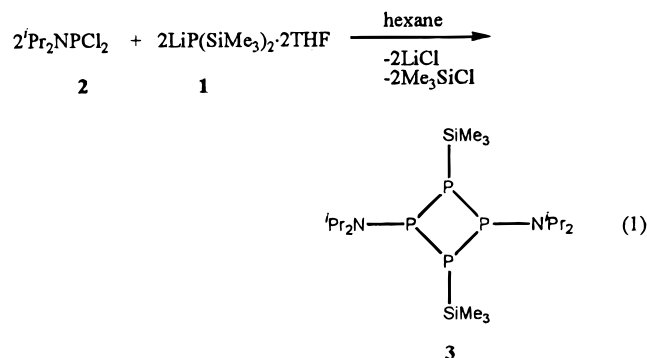
All calculations were performed on a Siemens SHELXTL PLUS

structure determination system.<sup>12</sup> Solutions for the data sets were by heavy atom (**4**) and direct methods (**11**) and full-matrix least-squares refinements were employed.<sup>13</sup> Neutral atom scattering factors and anomalous dispersion terms were used for all non-hydrogen atoms during the refinements. The function minimized was  $\sum w(|F_o| - |F_c|)^2$ . Hydrogen atoms were placed in idealized positions (riding model) with fixed isotropic  $U_{\text{iso}} = 1.25U_{\text{equiv}}$  of the parent atom. Compound **11** showed disorder in the  $\text{tBu}$  group on C(19). A disorder model with two sites, occupancies of 0.55 and 0.45, was employed.

## Results and Discussion

Fritz and co-workers<sup>3,4</sup> have partially described reactions of several organochlorophosphanes with  $\text{LiP}(\text{SiMe}_3)_2 \cdot 2\text{THF}$ . They noted that several products form depending upon reactant stoichiometries, reaction temperature, and subsequent thermal or photolytic treatment of the initially generated products. Illustrative transformations are outlined in Scheme 1 for  $\text{tBuPCL}_2$ .<sup>3</sup> Thermolysis or photolysis of the four-membered ring compound produced a series of polyphosphine cage compounds.<sup>3,4</sup> In a similar fashion, reaction of  $\text{Me}_2\text{NPCL}_2$  with  $\text{LiP}(\text{SiMe}_3)_2 \cdot 2\text{THF}$  produced a triphosphane,  $(\text{Me}_3\text{Si})_2\text{P}-\text{P}(\text{NMe}_2)-\text{P}(\text{SiMe}_3)_2$ , which apparently decomposed near  $20^\circ\text{C}$  giving several products including the four-membered ring compound  $[(\text{Me}_3\text{Si})_2\text{PPP}(\text{SiMe}_3)]_2$ .<sup>4</sup> Much of this chemistry remains incompletely described or elucidated so additional studies seem warranted.

In the present study, the 1:1 combination of  $\text{tPr}_2\text{NPCL}_2$  with  $\text{LiP}(\text{SiMe}_3)_2 \cdot 2\text{THF}$ , in hexane solution at  $23^\circ\text{C}$ , gives a good yield of the four-membered ring compound **3** as described in eq 1. Compound **3** is a yellow crystalline, slightly moisture-



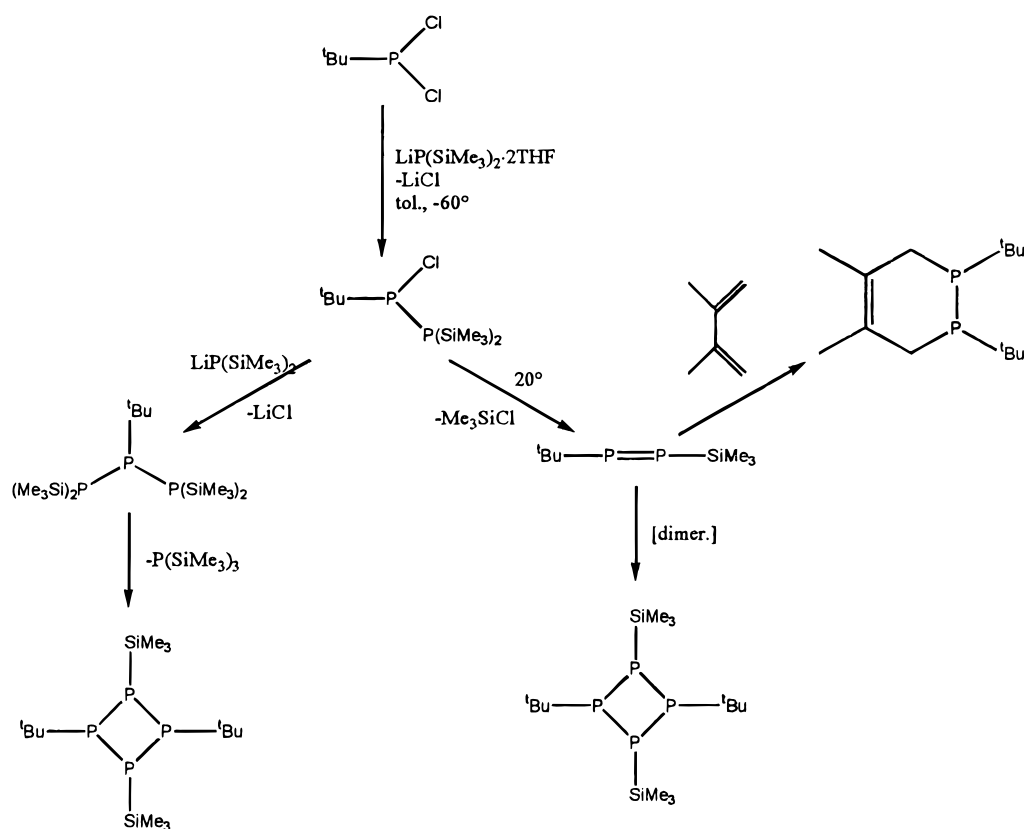
sensitive solid that is easily purified by sublimation. It displays a strong parent ion in its mass spectrum and provides satisfactory elemental (CHN) analyses. The NMR spectra for **3** are summarized in Table 2. The  $^3\text{1P}\{^1\text{H}\}$  NMR spectrum displays an AA'BB' type pattern, and it is shown in Figure 1 along with a simulated spectrum. The simulation provides the following parameters:  $\delta_A -36.1$ ,  $\delta_B -40.5$ , and  $^1J_{\text{AB}} = 161.0$  Hz. The

(10) Space group notation is given in *International Tables for X-Ray Crystallography*; Reidel: Dordrecht, Holland, 1983; Vol. I, pp 73–346.

(11) The empirical absorption corrections use an ellipsoidal model fitted to azimuthal scan data that are then applied to the intensity data: *SHELXTL Manual*, Revision 4; Nicolet XRD Corp.: Madison, WI, 1983.

(12) Sheldrick, G. M. *Nicolet SHELXTL Operations Manual*; Nicolet XRD Corp.: Cupertino, CA, 1981. SHELXTL uses absorption, anomalous dispersion, and scattering data compiled in *International Tables for X-Ray Crystallography*; Kynoch: Birmingham, England, 1974; Vol. IV, pp 55–60, 99–101, 149–150. Anomalous dispersion terms were included for all atoms with atomic numbers greater than 2.

(13) A general description of the least-squares algebra is found in *Crystallographic Computing*; Ahmed, F. R., Hall, S. R., Huber, C. P., Eds.; Munksgaard: Copenhagen, 1970; p 187. The least-squares refinement minimizes  $\sum w(|F_o| - |F_c|)^2$ , where  $w = 1/(\sigma(F)^2 + gF^2)$ .

Scheme 1<sup>3,4</sup>**Table 2.** NMR Data for Compounds **3**, **4**, **9**, **10**, and **11**

compd	<sup>31</sup> P	<sup>1</sup> H	<sup>13</sup> C
<b>3</b>	-36.1	0.43 [(CH <sub>3</sub> ) <sub>3</sub> Si]	0.14 [(CH <sub>3</sub> ) <sub>3</sub> Si]
	-40.5	1.17 (CH <sub>3</sub> )	23.9 (CH <sub>3</sub> )
	( <sup>1</sup> J <sub>PP</sub> = 161.0)	3.90 (CH)	48.5 (CH)
<b>4</b>	54.8 (t of d)	0.51 [(CH <sub>3</sub> ) <sub>3</sub> Si, d]	0.22 [(CH <sub>3</sub> ) <sub>3</sub> Si, m]
	9.1 (d of d)	( <sup>3</sup> J <sub>PH</sub> = 4.1 Hz)	24.0 (CH <sub>2</sub> )
	-38.5 (t of dt)	0.35 [(CH <sub>3</sub> ) <sub>3</sub> Si, d]	25.0 (CH <sub>3</sub> )
	( <sup>1</sup> J <sub>P(1)P(2)}</sub> = 277.4 Hz,	( <sup>3</sup> J <sub>PH</sub> = 4.1 Hz)	49.8 (CH, br)
	<sup>1</sup> J <sub>P(2)P(3)}</sub> = 133.2 Hz,	1.30 (CH <sub>3</sub> , d)	214.9 (CO)
	<sup>2</sup> J <sub>P(1)P(3)}</sub> = 89.4 Hz)	( <sup>4</sup> J <sub>PH</sub> = 6.6 Hz)	214.7 (CO)
<b>9</b>	111.9 (d)	1.01 (CH <sub>3</sub> , d)	3.0 (Me <sub>3</sub> Si)
	-175.9 (d)	( <sup>4</sup> J <sub>PH</sub> = 6.6 Hz)	( <sup>2</sup> J <sub>PC</sub> = 6.7 Hz,
	( <sup>1</sup> J <sub>PP</sub> = 155.4 Hz)	3.92 (CH, br)	<sup>3</sup> J <sub>PC</sub> = 3.8 Hz)
		0.36 (Me <sub>3</sub> Si)	3.17 (MeN)
		( <sup>3</sup> J <sub>PH</sub> = 3.5 Hz,	( <sup>2</sup> J <sub>PC</sub> = 4.3 Hz)
		<sup>4</sup> J <sub>PH</sub> = 0.6 Hz)	45.6 (MeN)
		3.11 (MeN)	( <sup>2</sup> J <sub>PC</sub> = 4.3 Hz)
<b>10</b>	217.3 (d)	0.53 (Me <sub>3</sub> Si)	4.0 (Me <sub>3</sub> Si)
	-127.8 (d)	1.32 (tBu)	29.2 (tBu)
	( <sup>1</sup> J <sub>PP</sub> = 436)		( <sup>3</sup> J <sub>CP</sub> = 7.7 Hz)
			55.0 ( <sup>2</sup> J <sub>CP</sub> = 17.8 Hz,
<b>11</b>	200.7 (d)	0.54 (Me <sub>3</sub> Si)	<sup>3</sup> J <sub>CP</sub> = 2.5 Hz)
	-82.0 (t)	1.43 (tBu)	2.8 (Me <sub>3</sub> Si, m)
	( <sup>1</sup> J <sub>PP</sub> = 525 Hz)		( <sup>2</sup> J <sub>CP</sub> = 8 Hz)
			28.8 (CH <sub>3</sub> , m)
			( <sup>3</sup> J <sub>CP</sub> = 3.7 Hz)
			55.0 (C, t)

<sup>1</sup>H and <sup>13</sup>C{<sup>1</sup>H} NMR data show single resonances attributed to the Si(CH<sub>3</sub>)<sub>3</sub>, <sup>i</sup>Pr methyl, and <sup>i</sup>Pr methine groups.

Subsequent combination of **3** with Fe<sub>2</sub>(CO)<sub>9</sub> in a 1:1 ratio in hexane gives a red-brown crystalline solid [<sup>i</sup>Pr<sub>2</sub>NPP(SiMe<sub>3</sub>)<sub>2</sub>]<sub>2</sub>·Fe(CO)<sub>4</sub>, **4**. Attempts to obtain a bis-Fe(CO)<sub>4</sub> complex by use of a 1:2 reactant ratio failed. The infrared spectrum of **4** in hexane solution displays three strong absorptions at 2039, 1965

and 1933 cm<sup>-1</sup>. The pattern is consistent with C<sub>3v</sub> local symmetry in a Fe(CO)<sub>4</sub>·L fragment for which three carbonyl stretching frequencies (2a + e) would be expected.<sup>14-16</sup> The band positions also are comparable to the values observed for Fe(CO)<sub>4</sub>·L complexes of phosphinoborane cage species, P<sub>2</sub>(Pr<sub>2</sub>NB)<sub>2</sub>(tms<sub>2</sub>NB) and P<sub>2</sub>(tmpB)<sub>2</sub>(Pr<sub>2</sub>NB) (tmp = 2,2,6,6-tetramethylpiperidino).<sup>17</sup> The <sup>31</sup>P{<sup>1</sup>H} NMR spectrum shows three resonances centered at δ 54.8, 9.1, and -38.5 in a 1:2:1 area ratio. The low and high field resonances are triplets of doublets and the middle resonance is a doublet of doublets. The resulting coupling parameters are: <sup>1</sup>J<sub>P(1)-P(2)}</sub> = 277.4 Hz, <sup>2</sup>J<sub>P(2)-P(2)}</sub> = 133.2 Hz, and <sup>2</sup>J<sub>P(1)-P(3)}</sub> = 89.4 Hz. The <sup>1</sup>H NMR spectrum shows two sets of doublets for the SiMe<sub>3</sub> and <sup>i</sup>Pr<sub>2</sub>N methyl groups; however, only one broad resonance is resolved for the methine hydrogen atoms. The <sup>13</sup>C{<sup>1</sup>H} spectrum shows a complex overlapping pattern (two partially overlapped triplets) centered at δ 0.22 for the inequivalent Me<sub>3</sub>Si groups, two equally intense peaks at δ 24.0 and 25.0 for the inequivalent <sup>i</sup>Pr<sub>2</sub>N methyl groups, a broad resonance at δ 49.8 for the <sup>i</sup>Pr<sub>2</sub>N methine groups, and two resonances in the carbonyl region, δ 214.9 and 214.7.

Potentially either the P-SiMe<sub>3</sub> or P-N<sup>i</sup>Pr<sub>2</sub> centers could act as Lewis bases toward an Fe(CO)<sub>4</sub> fragment, and the spectroscopic data do not provide an unambiguous probe of the coordination condition in **4**. As a result, the molecular structure was determined by single crystal X-ray diffraction techniques. A view of the structure is shown in Figure 2, and selected bond

(14) Darensbourg, D. J.; Nelson, H. H.; Hyde, C. L. *Inorg. Chem.* **1974**, *13*, 2135.

(15) Cowley, A. H.; Kemp, R. A.; Wilburn, J. C. *Inorg. Chem.* **1981**, *20*, 4289.

(16) Montemayor, R. G.; Sauer, D. T.; Fleming, S.; Bennett, D. W.; Thomas, M. G.; Parry, R. W. *J. Am. Chem. Soc.* **1978**, *100*, 2231.

(17) Dou, D.; Wood, G. L.; Duesler, E. N.; Paine, R. T.; Nöth, H. *Inorg. Chem.* **1992**, *31*, 3756.

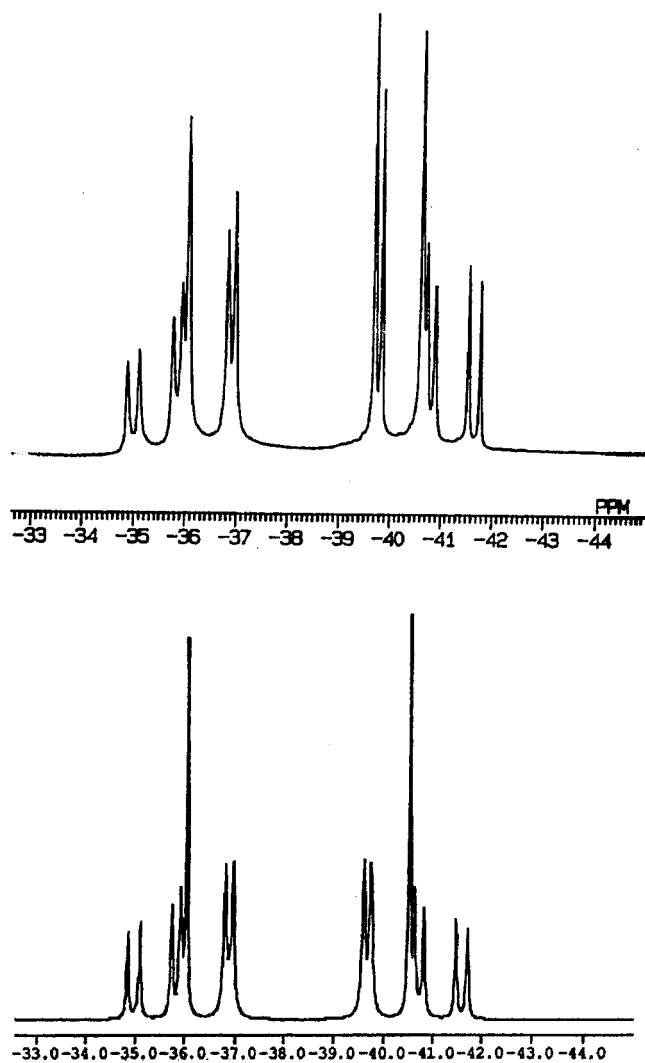


Figure 1.  $^{31}\text{P}\{^1\text{H}\}$  NMR spectrum for  $[\text{Pr}_2\text{NPP}(\text{SiMe}_3)]_2 \cdot \text{Fe}(\text{CO})_4$ , **3**: (a) measured spectrum; (b) simulated spectrum.

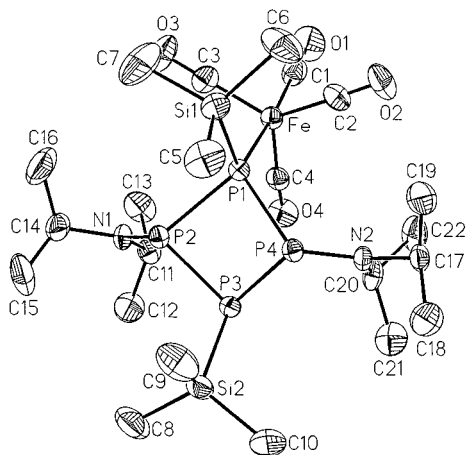


Figure 2. Molecular structure and atom labeling scheme for  $[\text{Pr}_2\text{NPP}(\text{SiMe}_3)]_2 \cdot \text{Fe}(\text{CO})_4$ , **4** (30% thermal ellipsoids).

lengths and angles are summarized in Table 3. It is found that the ligand four-membered ring is bonded to the  $\text{Fe}(\text{CO})_4$  through the phosphorus atom of the  $\text{P}(1)\text{—SiMe}_3$  group. The  $\text{P}_4$  ring is folded along the  $\text{P}(2)\cdots\text{P}(4)$  vector ( $\theta = 45.9^\circ$ ) and the two  $\text{SiMe}_3$  groups are in a *cis* configuration exo to the ring. The  $\text{Fe}(\text{CO})_4$  group is positioned over the cup of the fold. The  $\text{Pr}_2\text{N}$  groups are planar and nearly perpendicular to the  $\text{P}_4$  ring. The

Table 3. Selected bond lengths (Å) and angles ( $^\circ$ ) for  $[\text{Pr}_2\text{NPP}(\text{SiMe}_3)]_2 \cdot \text{Fe}(\text{CO})_4$ , **4** and  $[(\text{tBuNP})_2\text{P}(\text{SiMe}_3)]_2$ , **11**

<b>4</b>		<b>11</b>	
Bond Lengths			
P(1)—P(2)	2.294(2)	P(1)—P(2)	2.212(2)
P(2)—P(3)	2.222(2)	P(1)—P(6)	2.225(3)
P(3)—P(4)	2.219(2)	P(3)—P(4)	2.206(3)
P(1)—P(4)	2.283(2)	P(4)—P(5)	2.225(2)
P(1)—Si(1)	2.296(3)	P(1)—Si(1)	2.249(3)
P(3)—Si(2)	2.272(3)	P(4)—Si(2)	2.258(3)
P(2)—N(1)	1.673(5)	P(2)—N(1)	1.736(6)
P(4)—N(2)	1.673(5)	P(2)—N(2)	1.745(5)
		P(3)—N(1)	1.732(5)
		P(3)—N(2)	1.723(6)
		P(5)—N(3)	1.722(6)
		P(5)—N(4)	1.714(5)
		P(6)—N(3)	1.732(5)
		P(6)—N(4)	1.716(6)
Fe—P(1)	2.311(2)		
Bond Angles			
P(2)—P(1)—P(4)	84.0(1)	P(2)—P(1)—P(6)	123.9(1)
P(1)—P(2)—P(3)	84.8(1)	P(3)—P(4)—P(5)	124.2(1)
P(2)—P(3)—P(4)	87.3(1)		
P(3)—P(4)—P(1)	85.1(1)		
Si(1)—P(1)—P(2)	101.0(1)	Si(1)—P(1)—P(2)	107.8(1)
Si(1)—P(1)—P(4)	101.6(1)	Si(1)—P(1)—P(6)	106.5(1)
Si(2)—P(3)—P(2)	102.1(1)	Si(2)—P(4)—P(3)	105.8(1)
Si(2)—P(3)—P(4)	101.9(1)	Si(2)—P(4)—P(5)	108.2(1)
P(1)—P(2)—N(1)	114.9(2)	P(1)—P(2)—N(1)	102.0(2)
P(3)—P(2)—N(1)	104.5(2)	P(1)—P(2)—N(2)	110.4(2)
P(1)—P(4)—N(2)	113.5(2)	P(4)—P(3)—N(1)	101.4(2)
P(3)—P(4)—N(2)	106.8(2)	P(4)—P(3)—N(2)	111.4(2)
		P(2)—N(1)—P(3)	96.4(2)
		P(2)—N(2)—P(3)	96.4(2)
		N(1)—P(2)—N(2)	83.0(3)
		N(1)—P(3)—N(2)	83.8(2)
P(2)—P(1)—Fe	126.4(1)		
P(4)—P(1)—Fe	124.6(1)		

P—P bond distances fall into two groups:  $\text{P}(1)\text{—P}(2)$  2.294(2) Å and  $\text{P}(1)\text{—P}(4)$  2.283(2) Å;  $\text{P}(3)\text{—P}(2)$  2.222(2) Å and  $\text{P}(3)\text{—P}(4)$  2.219(2) Å. This is consistent with P—P bond weakening involving the Fe-coordinated P(1) center. These distances compare favorably with P—P distances in a variety of polyphosphine ring and cage compounds.<sup>18</sup> In addition, the  $\text{P}(1)\text{—Si}(1)$  distance, 2.296(3) Å, is slightly longer than the  $\text{P}(3)\text{—Si}(2)$  distance, 2.272(3) Å. The  $\text{P}(1)\text{—Fe}$  bond length, 2.311(2) Å, is significantly longer than the coordinate bond length in  $\text{Ph}_3\text{P}\cdot\text{Fe}(\text{CO})_4$ , 2.244(1) Å.<sup>19</sup> The coordination geometry about the Fe atom can be considered trigonal bipyramidal, with the P(1) atom *trans* to C(1); the  $\text{P}(1)\text{—Fe—C}(1)$  angle is  $172.1(3)^\circ$ . The exo P—N $\text{Pr}_2$  bond length, 1.673(5) Å, is moderately short, and it can be compared with the exo P—N distances in the diphosphane  $[(\text{Me}_3\text{Si})_2\text{N}(\text{Ph})\text{P}]_2$  1.724(4) Å,<sup>20</sup> and the diazaphosphiridine  $\text{tBuN}(\text{tBu})\text{NPN}\text{Pr}_2$  1.669(5) Å.<sup>21</sup>

The 2:1 combination  $(\text{Me}_3\text{Si})_2\text{PLi}\cdot 2\text{THF}$  with  $\text{Pr}_2\text{NPPCl}_2$  was also examined and found to produce **3** and  $\text{P}(\text{SiMe}_3)_3$  as described in Scheme 1 for  $\text{tBuPCL}_2$ . A very small amount of a second product, with  $^{31}\text{P}$  NMR resonances at  $\delta$  62 and 195, was also formed. These resonances may result from the acyclic triphosphane  $[(\text{Me}_3\text{Si})_2\text{P}]_2\text{PN}\text{Pr}_2$ ; however, this material was not isolated and fully characterized. In an effort to trap the possible intermediate species  $\text{Pr}_2\text{NP}=\text{PSiMe}_3$ , the reaction of  $\text{Pr}_2\text{NPPCl}_2$  and  $\text{LiP}(\text{SiMe}_3)_2\cdot 2\text{THF}$  was performed in hexane solution in the presence of 1 equiv of 2,3-dimethyl-1,3-

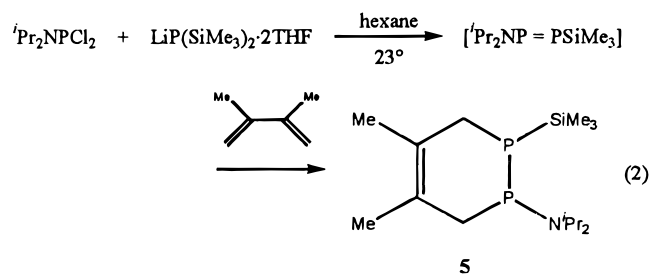
(18) Baudler, M.; Glinka, K. In *The Chemistry of Inorganic Homo- and Heterocycles*; Haiduc, I., Sowerby, D. B., Eds.; Academic Press: New York, 1987; Vol. II, Chapter 18.

(19) Riley, P. E.; Davis, R. E. *Inorg. Chem.* **1980**, *18*, 159.

(20) McNamara, W. F. Ph.D. Thesis, University of New Mexico, 1987.

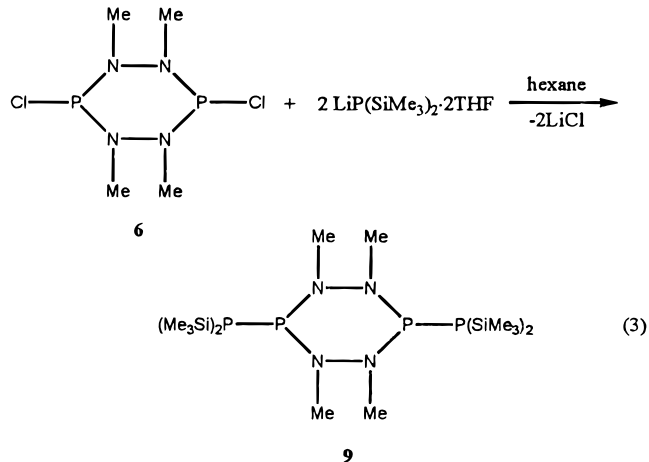
(21) Niecke, E.; Schwichtenhövel, K.; Schäfer, H.-G.; Krebs, B. *Angew. Chem., Int. Ed. Engl.* **1981**, *20*, 963.

butadiene. The resulting chemistry is summarized in eq 2. The



${}^{31}\text{P}\{^1\text{H}\}$  NMR spectrum shows the second order pattern described above for **3**, but it also contains two doublets centered at  $\delta$  25.0 and  $-120.3$  with  ${}^1J_{\text{PP}} = 244.1$  Hz which are tentatively ascribed to **5**. Based upon peak intensities, **5** is present in about 30% yield. Attempts to separate **5** from **3** were unsuccessful. An IR spectrum of the product mixture shows an absorption at  $1703\text{ cm}^{-1}$  which is assigned to a  $-\text{C}=\text{C}-$  stretch. There are no absorptions in this region for pure **3**. The  ${}^{13}\text{C}\{^1\text{H}\}$  NMR spectrum of the product mixture contains the three strong resonances already assigned to **3** as well as weak resonances at  $\delta$  48.5, 24.6, and 4.13.

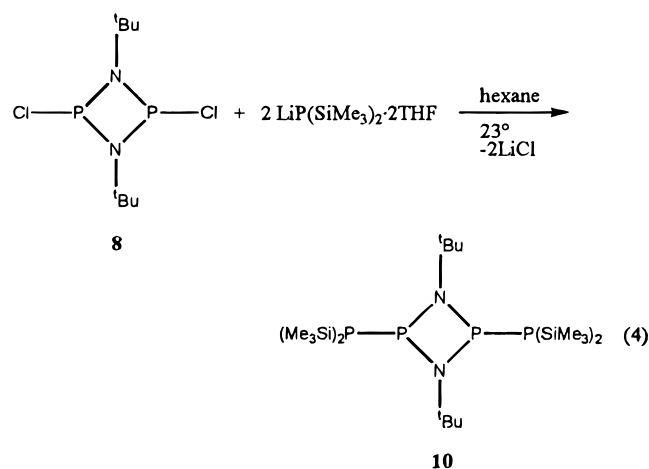
We are also interested in the use of cyclic aminohalophosphanes as possible cage structure building blocks; therefore, the reactions of three such reagents,  $\text{ClP}[\text{N}(\text{Me})\text{N}(\text{Me})_2]\text{PCl}$  (**6**),  $({}^i\text{PrNPCl}_2)_2$  (**7**), and  $({}^t\text{BuNPCl}_2)_2$  (**8**) with  $\text{LiP}(\text{SiMe}_3)_2 \cdot 2\text{THF}$  were examined. In the first case, combination of **6** with 2 equiv of  $\text{LiP}(\text{SiMe}_3)_2 \cdot 2\text{THF}$  in hexane at  $23^\circ\text{C}$  gave a colorless crystalline solid identified as the bis-substitution product **9**. This chemistry is summarized in eq 3. The compound does not



provide a parent ion in the EI mass spectrum; however, it gave satisfactory elemental analysis. The compound is air-sensitive and somewhat unstable in benzene. The  ${}^{31}\text{P}\{^1\text{H}\}$  NMR spectrum shows two equal intensity doublets centered at  $\delta$  111.9 and  $-175.9$  with  ${}^1J_{\text{PP}} = 155.4$  Hz. The low-field resonance is assigned to the  $-\text{PN}_2$  fragment and the high-field resonance to the  $-\text{P}(\text{SiMe}_3)_2$  fragment based upon well-defined shift regions for related aminophosphanes and silylphosphanes.<sup>22,23</sup> The  ${}^{13}\text{C}\{^1\text{H}\}$  NMR spectrum is simple showing a doublet of doublets at  $\delta$  3.0,  ${}^2J_{\text{PC}} = 6.7$  Hz,  ${}^3J_{\text{PC}} = 3.8$  Hz assigned to the trimethylsilyl carbon atoms and two doublets of doublets at  $\delta$

46.3 and 45.6,  ${}^2J_{\text{PC}} = 4.3$  Hz that are assigned to inequivalent hydrazino methyl groups. The  ${}^1\text{H}$  NMR spectrum consists of a doublet of doublets at  $\delta$  0.36,  ${}^3J_{\text{PH}} = 3.5$  Hz,  ${}^4J_{\text{PH}} = 0.6$  Hz, due to the  $\text{P}(\text{SiMe}_3)_2$  groups and two doublets of doublets centered at  $\delta$  3.17,  ${}^3J_{\text{PH}} = 1.5$  Hz,  ${}^4J_{\text{PH}} = 0.5$  Hz and at  $\delta$  3.11,  ${}^3J_{\text{PH}} = 1.6$  Hz,  ${}^4J_{\text{PH}} = 0.7$  Hz assigned to inequivalent hydrazino methyl groups. These properly integrate in a 6:1:1 ratio. The reaction was also run in a 1:1 reactant ratio in an effort to form the monosubstitution product; however, only **9** is found and in reduced yield.

The reaction of diazadiphosphetidine  $({}^i\text{Pr}_2\text{NPCl}_2)_2$  **7** with  $\text{LiP}(\text{SiMe}_3)_2 \cdot 2\text{THF}$  gives a variety of unidentified products; however, reactions with  $({}^t\text{BuNPCl}_2)_2$  **8** and the silylphosphide are efficient. The 1:2 combination gave a yellow, crystalline disubstitution product **10** in high yield as summarized in eq 4.



The mass spectrum of **10** does not contain a parent ion, but CHN analyses provide adequate composition characterization. The NMR data for **10** are consistent with the proposed structure. Similar with **9**, the  ${}^{31}\text{P}$  NMR spectrum of **10** displays two doublets of equal intensity at  $\delta$  217.3 and  $-127.8$  with  ${}^1J_{\text{PP}} = 436$  Hz. The low-field resonance is assigned to the ring  $-\text{PN}_2$  phosphorus atoms and the high field resonance is assigned to the exo  $-\text{PSi}_2$  phosphorus atoms. The  ${}^1\text{H}$  NMR spectrum contains a single resonance at  $\delta$  1.32 assigned to the  ${}^t\text{Bu}$  methyl groups and a "pseudo triplet" centered at  $\delta$  0.53 assigned to the  $\text{P}(\text{SiMe}_3)_2$  groups. As expected, these peaks integrate with a 1:2 ratio. The  ${}^{13}\text{C}\{^1\text{H}\}$  NMR spectrum shows a resonance centered at  $\delta$  55.0 that is split into a triplet of triplets,  ${}^2J_{\text{CP}} = 17.8$  Hz,  ${}^3J_{\text{CP}} = 2.5$  Hz, that is attributed to the  $\text{Me}_3\text{C}$  atom. The  ${}^t\text{Bu}$  methyl groups display a triplet at  $\delta$  29.2 with  ${}^3J_{\text{CP}} = 7.7$  Hz, and the  $\text{Me}_3\text{Si}$  groups produce a "pseudo-quartet" centered at  $\delta$  4.0.

Extensive studies of 1,3,2,4-diazadiphosphetidines,  $(\text{XPNR})_2$ , have shown that these four-membered ring compounds form with either or both cis and trans geometries.<sup>24,25</sup> For  $\text{N}(\text{ring})$ -alkyl-substituted derivatives,  $\text{R} = \text{alkyl}$ , the cis isomer is normally dominant or completely favored in reaction mixtures. This has been demonstrated with a variety of phosphorus substituent groups,  $\text{X} = \text{halo}$ , alkoxy, dialkylamino,<sup>24,25</sup> and monoalkylamino<sup>26</sup> by use of  ${}^{31}\text{P}$  NMR shifts and X-ray crystallographic data. In general, it is found that the  ${}^{31}\text{P}$  NMR shift for the cis isomer lies downfield from the trans isomer,

(22) Tebby, J. C. In *Phosphorus-31 NMR Spectroscopy in Stereochemical Analysis*; Verkade, J. G., Quin, L. D., Eds.; VCH Publishers, Inc.: Deerfield Beach, FL, 1987.

(23) Crutchfield, M. M.; Dungan, C. H.; Letcher, J. H.; Mark, V.; Van Wazer, J. R. *Top. Phosphorus Chem.* **1967**, 5, 1.

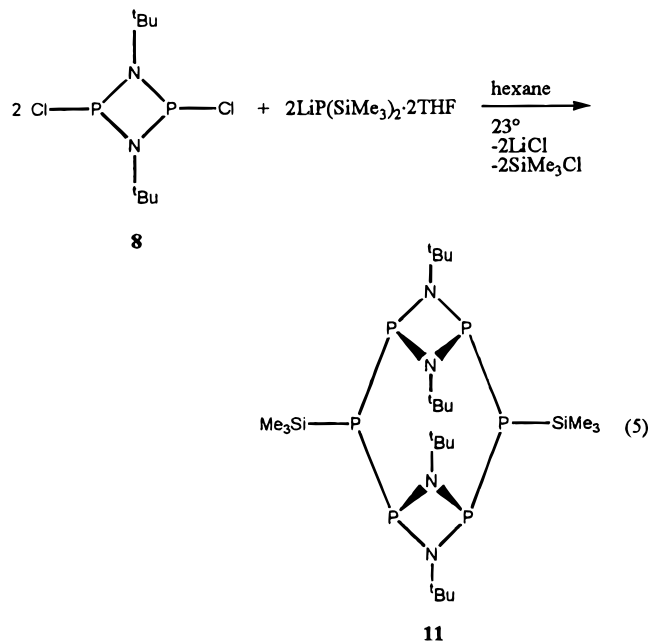
(24) Bulloch, G.; Keat, R.; Thompson, D. G. *J. Chem. Soc., Dalton Trans.* **1977**, 99 and references therein.

(25) Keat, R. *Top. Curr. Chem.* **1982**, 102, 89.

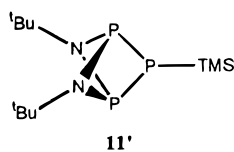
(26) Chen, H. J.; Haltiwanger, R. C.; Hill, T. G.; Thompson, M. L.; Coons, D. E.; Norman, A. D. *Inorg. Chem.* **1985**, 24, 4725.

and in some cases the shift difference is large (50–100 ppm). Reaction mixtures containing **10** show only two resonances,  $\delta$  217.3 for  $-\text{PN}_2$  and  $-127.8$  for  $-\text{P}(\text{SiMe}_3)_2$ . Hence, it is concluded that only one isomer forms. Given the significant downfield shift of the resonance attributed to the  $-\text{PN}_2$  groups in the 1,3,2,4-diazoadiphosphetidine ring, it is proposed that **10** is formed only as the cis isomer. Support for this assignment is also provided by the  $^{31}\text{P}$  NMR data for **11**, which are discussed below. In **11**, the four-membered  $\text{P}_2\text{N}_2$  rings must exist in a cis conformation.

The 1:1 reaction of **8** with  $\text{LiP}(\text{SiMe}_3)_2 \cdot 2\text{TTHF}$  in hexane at  $23^\circ\text{C}$  gives a particularly interesting result summarized in eq 5. Compound **11** [ $(^t\text{BuNP})_2\text{P}(\text{SiMe}_3)_2$ ] is isolated in 24% yield



as an orange crystalline solid; however, a significant amount remains dissolved in hexane.  $^{31}\text{P}$  NMR data for the reaction mixture suggests that **11** is produced in greater than 85% yield. A mass spectrum of the product shows a weak parent ion at  $m/e$  616 consistent with the “dimer structure” **11**. No peak is seen at  $m/e$  308, which would correspond to a monomer species that might be expected to have a closo structure such as represented by **11'**. The NMR data for this molecule are



complex. The  $^{31}\text{P}\{^1\text{H}\}$  NMR spectrum shows two second-order patterns centered at  $\delta$  200.7 and  $-82.0$  in a 2:1 ratio. The lower field resonance is a second-order  $\text{A}_2\text{X}$  “doublet” that may be attributed to the  $-\text{PN}_2$  groups. The low field shift is comparable to that of **10** and it is consistent with a cis geometry in the  $\text{P}_2\text{N}_2$  ring. The higher field resonance is a “triplet” that is assigned to the  $-\text{PTMS}$  bridging groups. The  $^1\text{H}$  NMR spectrum is similar to that of **10** with a single resonance at  $\delta$  1.43 ( $^t\text{Bu}$ ) and a “pseudo triplet” at  $\delta$  0.54 in a 2:1 area ratio. The  $^{13}\text{C}\{^1\text{H}\}$  NMR spectrum contains resonances at  $\delta$  55.0 ( $\text{Me}_3\text{C}$ ), 28.8 ( $\text{H}_3\text{CC}$ ), and 2.8 ( $\text{H}_3\text{CSi}$ ). Each of these resonances has complex, overlapping coupling patterns that have not yet been fully resolved.

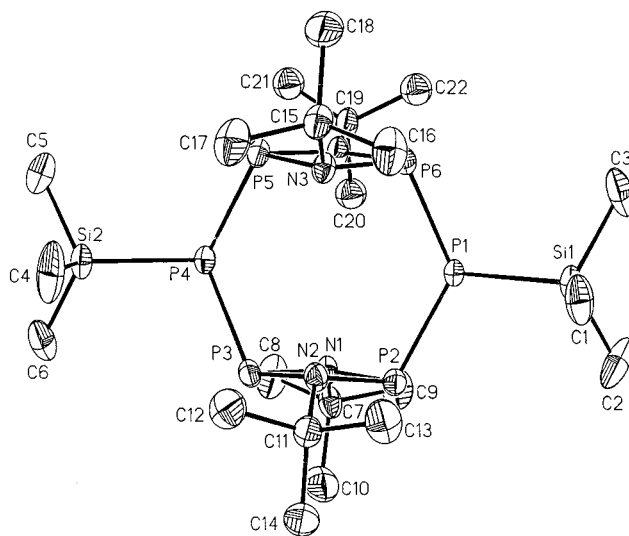


**Figure 3.** Molecular structure and atom labeling scheme for  $[(^t\text{BuNP})_2\text{P}(\text{SiMe}_3)_2]$ , **11** (30% thermal ellipsoids).

The proposed dimer structure of **11** has been confirmed by single crystal X-ray diffraction analysis, and a view of the molecule is shown in Figure 3. The structure consists of two planar  $\text{P}_2\text{N}_2$  diazoadiphosphetidine fragments stacked in an eclipsed orientation. The rings are joined to each other through two bridging  $\text{PSiMe}_3$  groups. The resulting cage structure is reminiscent of the low-temperature structure of  $\text{P}_4(\text{N}^i\text{Pr}_2)_6$  **12** which contains two  $(\text{P}_2\text{N}^i\text{Pr}_2)$  rings stacked on top of each other, linked P to P' by bridging  $^i\text{Pr}_2\text{N}$  groups.<sup>27</sup> In **11**, the exo  $^t\text{Bu}$  groups on the  $\text{P}_2\text{N}_2$  rings have a cis relationship, and they are pushed back away from the interior of the cage. Interestingly, the two terminal  $\text{Me}_3\text{Si}$  groups are also cis to each other. The average P–N distances in the  $\text{P}_2\text{N}_2$  rings is 1.728(6) Å (range: 1.714(5)–1.745(5) Å) which is comparable with the value in **12**, 1.70(1) Å. The average P–P bridging distance, 2.217(3) Å, is comparable with P–P distances in a variety of polyphosphanes.<sup>18</sup> Finally, the nonbonded  $\text{P}_2 \cdots \text{P}_3$  and  $\text{P}_5 \cdots \text{P}_6$  distances, 2.586(3) and 2.589(3) Å, are relatively short.

The chemistry outlined here between  $\text{LiP}(\text{SiMe}_3)_2 \cdot 2\text{TTHF}$  and various aminochlorophosphanes has some resemblance to the chemistry found with organochlorophosphanes;<sup>3,4</sup> however, some interesting differences are also revealed. In particular, the new compounds appear to be more stable toward degradation with subsequent polyphosphane formation although extended heating of **3**, **4**, **9**, and **10** has not been attempted. Finally, the reactivity of the halodiazoadiphosphetidines has provided an unexpected pathway to the cage molecule **11**, and this chemistry suggests routes to new cages containing other aminophosphane and  $\text{PSiMe}_3$  and PH fragments.

**Acknowledgment** is made to the National Science Foundation (Grant CHE-9508668) for support of this research.

**Supporting Information Available:** Tables containing heavy atom coordinates, anisotropic thermal parameters, hydrogen atom coordinates, and complete listings of bond distances and angles. This material is available free of charge via the Internet at <http://pubs.acs.org>.

IC980954E